


 Cite this: *RSC Adv.*, 2020, 10, 10606

# Highly-selective solvent-free catalytic isomerization of $\alpha$ -pinene to camphene over reusable titanate nanotubes

 Geng Huang,<sup>a</sup> Shuolin Zhou,<sup>b</sup> Jian Liu,<sup>a</sup> Shengpei Su<sup>\*a</sup> and Dulin Yin<sup>\*a</sup>

Titanate nanotubes, prepared by the hydrothermal reconstitution and modification with hydrochloric acid, were tested as solid acid catalysts in the isomerization of  $\alpha$ -pinene under solvent free conditions. The results showed that titanate nanotubes have better catalytic properties than titanium dioxide nanoparticles, and the camphene was the main product for  $\alpha$ -pinene isomerization. The effects of several reaction variables, such as reaction temperature, catalyst dosage, and reaction time, on the conversion of  $\alpha$ -pinene and the selectivity to camphene were examined. The highest conversion was up to 97.8% with selectivity to camphene of 78.5% under the mild reaction conditions, and the catalyst also showed outstanding reusability after four runs. It is proposed that appropriate surface acidic sites and opened nanotubular structures are mainly responsible for the excellent catalytic performance of titanate nanotubes materials.

 Received 5th February 2020  
 Accepted 9th March 2020

DOI: 10.1039/d0ra01093f

[rsc.li/rsc-advances](http://rsc.li/rsc-advances)

## Introduction

The production of high value-added chemicals from biomass has attracted a lot of attention.<sup>1</sup>  $\alpha$ -Pinene extracted from resin tapping, wood pulp papermaking and cellulose production is an inexpensive and important essential oil, which is widely used in the synthesis of various fine chemicals. Many research works indicated that  $\alpha$ -pinene can be rearranged to give several isomeric products in the presence of an acid catalyst. Among several isomers, camphene is especially important substrate in the production of fragrance materials, acrylates, terpene-phenol resins and other chemical derivatives.<sup>2</sup> Camphene is also a key intermediate from  $\alpha$ -pinene for the production of isobornyl esters and camphor which are extensively used as mildew proofing and insecticidal agents in our daily life.

Camphene is generally obtained by the isomerization of  $\alpha$ -pinene using acidic catalysts. In recent years, the use of heterogeneous catalyst is a shift toward green and environmental-friendly technologies. Various solid acid catalysts, such as zeolites,<sup>3,4</sup> iron-modified zeolites,<sup>5</sup> sulfated zirconia,<sup>6</sup> modified layered aluminosilicates,<sup>7</sup> Al-incorporated MCM-41,<sup>8</sup> MSU-S mesoporous materials,<sup>9</sup>  $W_2O_3/Al_2O_3$ ,<sup>10</sup> phosphotungstic heteropoly acids,<sup>11</sup> Ti-SBA-15 (ref. 12 and 13), and ionic liquids<sup>12</sup> have been employed for the isomerization of  $\alpha$ -

pinene. However, there is still a challenge to develop new catalysts which possess higher activity and selectivity to camphene during the  $\alpha$ -pinene isomerization process.

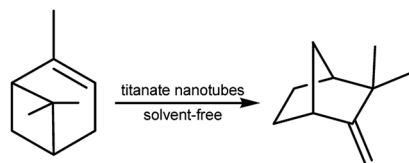
In recent years, titanium dioxide nanoparticles (TNPs) were worked as efficient catalyst for the acceleration of various organic reactions including Knoevenagel condensations,<sup>13</sup> Friedel–Crafts alkylation of indoles,<sup>14</sup> the aldol condensation of furfural,<sup>15</sup> Mannich synthesis of  $\beta$ -aminocarbonyls,<sup>16</sup> and synthesis of tetrahydrobenzo[*b*]pyran derivatives,<sup>17</sup>  $\alpha$ -amino-phosphonates<sup>18</sup> and polyhydroquinoline derivatives.<sup>19</sup> However, the weak acidity sites on the surface of TNPs are become a major drawback that limits the catalytic applications of TNPs in organic reactions. It has been reported that the reaction rate on titanium dioxide nanoparticles is low for the  $\alpha$ -pinene isomerization to camphene.<sup>20</sup> Surface modification of  $TiO_2$  materials with acidic groups is an efficient method to increase the catalytic activity.<sup>23,24</sup> Besides, textural properties are usually a factor influencing the activity of acid catalysts. Among titanium dioxide materials, one dimensional titanate nanotubes (TNTs) have novel properties such as large surface area and tubular structure that increase the number of active sites.<sup>21</sup> TNTs can be synthesized in large quantities *via* the hydrothermal treatment using commercial  $TiO_2$  powder. The main hollow tunnel structures are formed after the acid washing step that removing the  $Na^+$  ion to form Ti–OH bonds. This means that the surface acidity can be modified to tune the catalytic activity of TNTs during the acid washing process.

In the present work, titanate nanotubes were modified by different acids as solid catalysts to improve the isomerization of  $\alpha$ -pinene to camphene (Scheme 1). Repetition reuses were conducted in order to suit the catalyst's potential application.

<sup>a</sup>National & Local Joint Engineering Laboratory for New Petro-chemical Materials and Fine Utilization of Resources, Key Laboratory of Resource Fine-Processing and Advanced Materials of Hunan Province, Key Laboratory of Chemical Biology and Traditional Chinese Medicine Research (Ministry of Education of China), College of Chemistry and Chemical Engineering, Hunan Normal University, Changsha, 410081, P. R. China. E-mail: [sushengpei@yahoo.com](mailto:sushengpei@yahoo.com); [dulinyin@126.com](mailto:dulinyin@126.com); Fax: +86-731-88872531; Tel: +86-731-88872530

<sup>b</sup>College of Education, Changsha Normal University, Changsha, 410100, P. R. China





Scheme 1 The isomerization of  $\alpha$ -pinene over titanate nanotubes.

## Experimental

### Materials

TiO<sub>2</sub> nanoparticles (anatase, >99.9%) and  $\alpha$ -pinene were purchased from Aladdin and were used as received. Other chemical reagents, such as NaOH, HCl, H<sub>2</sub>SO<sub>4</sub>, HNO<sub>3</sub>, hexane, and ethanol were of analytical grade and used without further purification.

### Preparation of catalyst

TNTs were synthesized by the hydrothermal method in NaOH solution using commercial TNPs as Ti source referring to the previous work with some modifications.<sup>22</sup> 3 g TNPs were uniformly dispersed in 120 mL of 10 mol L<sup>-1</sup> NaOH aqueous solution, followed by hydrothermal treatment at 150 °C in a Teflon-lined autoclave for 24 h. The white powders were washed thoroughly with distilled water and 0.1 mol L<sup>-1</sup> [H<sup>+</sup>] HCl aqueous solution. Then, the suspension was centrifuged and the solid sample was washed with distilled water until the pH of the rinsing solution close to 7, and subsequently dried overnight under vacuum at 60 °C, the product denoted as TNTs-Cl. Similarly, TNTs-SO<sub>4</sub> and TNTs-NO<sub>3</sub> were prepared with 0.1 mol L<sup>-1</sup> H<sub>2</sub>SO<sub>4</sub> and HNO<sub>3</sub> aqueous solution during the acid washing process, respectively.

### Characterization

Prior to measurement, all samples were dried under vacuum. Fourier transform infrared spectrum (FT-IR) was obtained by the KBr pellet technique on a Nicolet 370 infrared spectrophotometer in the range 400–4000 cm<sup>-1</sup>. The crystalline structure of TNTs was determined by X-ray diffraction (XRD) spectroscopy using Bruker diffractometer with Cu K $\alpha$  wavelength ( $\lambda = 1.5418 \text{ \AA}$ ) and diffraction angle ( $2\theta$ ) ranging from 10–90°. The microscopic morphology of TNTs was investigated by using transmission scanning microscopy (TEM, JEOL 2100, Japan) and scanning electron microscope (SEM, Carl Zeiss Sigma-HD, Germany). The N<sub>2</sub> adsorption-desorption isotherms was recorded with an ASAP 2400 physisorption instrument made by Micromeritics Corporation (United States). Surface acidity of sample was determined from the adsorbed pyridine in hexane solution by ultraviolet spectrum (Shimadzu UV-1900, Japan).<sup>23</sup>

### Catalytic testing

The isomerization reaction was carried out in a 5 mL round bottom flask equipped with a condenser. In a typical run, 0.050 g catalyst and 1.0 mL of  $\alpha$ -pinene were added to the round bottomed flask and stirred for 5 min, and heated in

a thermostatic oil bath at atmospheric pressure. Once the reaction finish, the products were taken, centrifuged and analyzed quantitatively by gas chromatography. The products of the isomerization were identified by GC-MS analyses.

## Results and discussion

### Catalytic performance of modified TNTs in isomerization

The catalytic performance of TNPs and different TNTs was evaluated in the isomerization of  $\alpha$ -pinene under solvent free conditions, and the results have been summarized in Table 1. It was found that  $\alpha$ -pinene conversion was almost zero for 6 h at 100 °C in the blank experiment (Table 1, Entry 1), and the similar result was obtained for reaction using the commercial TNPs (Table 1, Entry 2). However, when modified TNTs materials were used as catalyst, an increase on the conversion of  $\alpha$ -pinene was observed (Table 1, Entry 3–5). It was found that the highest conversion of  $\alpha$ -pinene was 42.8% with 64.8% highest camphene selectivity when catalyzed by TNTs-Cl for only 120 min (Table 1, Entry 5). From the adsorption of pyridine, the surface acidity of modified TNTs was quantified in Table 1. The amount of acidity on the sample surface is related to the kind of acid agent. This means that the acid catalytic sites can be modified by mineral acid in the washing step. The improvement on the catalytic performance of TNTs can be explained as TNTs has Lewis acids sites and Brønsted acid sites,<sup>24</sup> and the strength distribution of acid sites are also adjusted by modifying the surface with different mineral acid. Lewis acid sites were mainly promoted when HCl was used in the washing step.<sup>24</sup> Interestingly, we found that the major product after the reaction was camphene, thus suggesting the appropriate surface acidic sites of TNTs-Cl play a determinant role in the selective isomerization reaction for enlarging the four number ring of  $\alpha$ -pinene to bicyclic camphene. The amount of acid sites of TNTs-NO<sub>3</sub> and TNTs-SO<sub>4</sub> are 0.46 and 0.58 mmol g<sup>-1</sup>, respectively. It is deduced that the stronger Brønsted acidic sites exist on the surface of TNTs-SO<sub>4</sub> and TNTs-NO<sub>3</sub>, so more monocyclic isomers, such as limonene and terpinolene are formed from cracking the four number ring of  $\alpha$ -pinene. The higher conversion of  $\alpha$ -pinene was obtained after 6 h and is 77.7% with 76.2% of selectivity for camphene over TNTs-Cl (Table 1, Entry 6).

Table 1 Catalytic performance of modified TNTs in  $\alpha$ -pinene isomerization<sup>a</sup>

Entry	Catalyst	Acidity (mmol g <sup>-1</sup> )	Time (min)	Conversion (%)	Selectivity (%)
1	—	—	360	—	—
2	TNPs	—	240	1.3	70.6
3	TNTs-NO <sub>3</sub>	0.46	120	15.2	52.3
4	TNTs-SO <sub>4</sub>	0.58	120	18.7	46.8
5	TNTs-Cl	0.83	120	42.8	64.8
6	TNTs-Cl	—	360	77.7	76.2

<sup>a</sup> Reaction conditions: 1 mL  $\alpha$ -pinene, 0.05 g catalyst, reaction temperature 100 °C.

### Catalyst characterization

Modified TNTs materials were identified by FT-IR analysis, and the corresponding FT-IR spectra are depicted in Fig. 1. The FT-IR spectra of the three samples were similar. For TNTs samples, the broad peak present at around 3214–3600  $\text{cm}^{-1}$  can be assigned the surface –OH stretching vibrations. The peak at 1638  $\text{cm}^{-1}$  arises from the O–H deformation vibration of H–O–H as well as Ti–OH bonds. The band at 1384  $\text{cm}^{-1}$  can be attributed to the Ti–O–H deformation vibration.<sup>25</sup> In addition, the peak around 477–486  $\text{cm}^{-1}$  in the spectrum could be same to interpret as the crystal lattice vibration of  $\text{TiO}_6$  octahedra.<sup>26</sup>

The XRD patterns of the TNTs-Cl, TNTs- $\text{SO}_4$  and TNT- $\text{NO}_3$  samples were recorded, and the results are presented in Fig. 2. The peaks at  $2\theta = 10.8^\circ$ ,  $24.5^\circ$ ,  $28.6^\circ$  and  $48.5^\circ$  which are still consistent with the characteristic diffraction signals of titanate nanotubes,<sup>30</sup> the main structure is not changed by the acid agent. Furthermore, the XRD patterns of the TNTs-Cl and TNTs- $\text{SO}_4$  showed a little change in the peaks.

TEM image of TNTs-Cl is shown in Fig. 3. It can be observed from Fig. 3a that the as-prepared titanium dioxide nanotubes are interlaced with each other, and nanotubes can be several micrometers in length. TNTs-Cl showed the nanotubes with openings at the ends. Titanium dioxide nanotubes have a hollow tubular structure with an internal diameter of about 9 nm, which is consistent with the reported literature. The morphology and structure of TNTs-Cl were further surveyed by SEM. It can be seen from the Fig. 3b that it is consistent with the above TEM observations.

The textural property of TNTs-Cl was further investigated using  $\text{N}_2$  adsorption–desorption isotherms, and the results are present in Fig. 4. TNTs-Cl has the type IV isotherms based on IUPAC classification, which is characteristic of the mesoporous materials. TNPs are non porous materials. The surface area value of TNTs-Cl was calculated by BET method to be 295  $\text{m}^2 \text{g}^{-1}$ . Besides, the pore volume of TNTs-Cl was 0.646  $\text{cm}^3 \text{g}^{-1}$ . At the same time, the results of pore size distribution of TNTs-Cl by BJH method, which can support the observation of TEM image. It can be clearly seen that the hydrothermal reconstitution method and post-modification method can be used to transform nanoparticles into nanotubes, which increases the surface area of the material. The opened hollow structure can

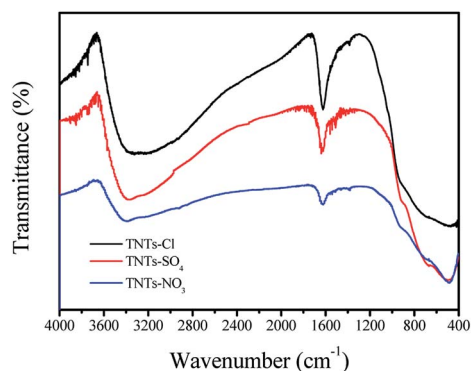


Fig. 1 FT-IR spectra of modified TNTs.

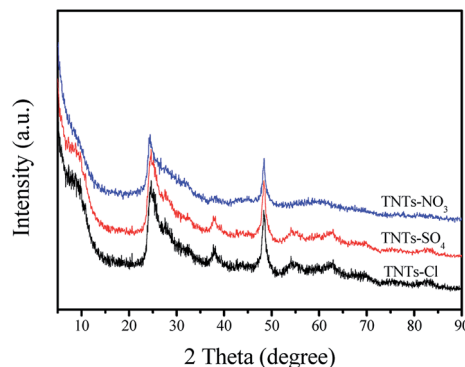


Fig. 2 XRD patterns of modified TNTs.

facilitate the contact of the substrate molecules with the active sites during the catalytic reaction process.

### Effect of isomerization condition

To check the variables such as reaction temperature, catalyst dosage, and reaction time effect on the results of the reaction, a series of single-factor experiment were performed using the best TNTs-Cl catalyst. Firstly, the conversion of  $\alpha$ -pinene and the selectivity of camphene were investigated as a function of temperature at a catalyst amount of 0.05 g between 90 and 130  $^\circ\text{C}$ , and the results are presented in Fig. 5.

It can be seen that an increase of the reaction temperature caused a significant increase in the conversion of  $\alpha$ -pinene. For the lower temperatures of 90  $^\circ\text{C}$ , the values of  $\alpha$ -pinene conversion were quite low and were 19.0%. The higher conversion of  $\alpha$ -pinene was obtained when the reaction temperature reached 100  $^\circ\text{C}$ . It was observed that a greater

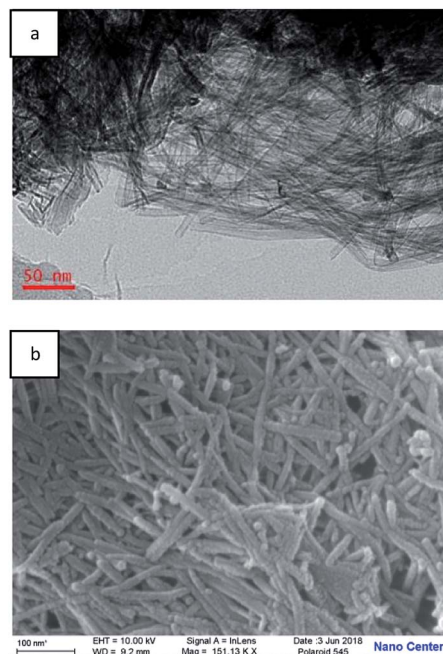


Fig. 3 TEM image (a) and SEM photographs (b) of TNTs-Cl.

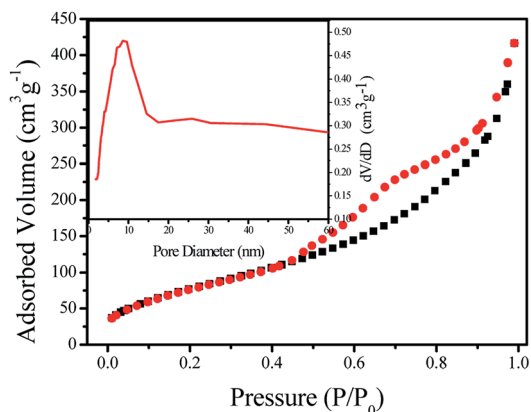


Fig. 4 Nitrogen adsorption–desorption isotherms for TNTs-Cl.

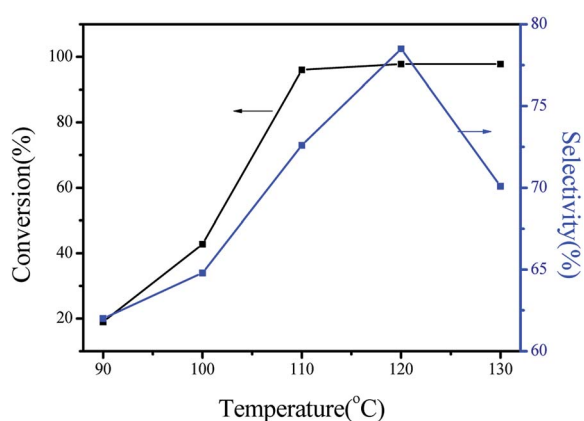


Fig. 5 Effect of the temperature in the catalytic performance of TNTs-Cl. Reaction conditions: 1 mL  $\alpha$ -pinene, 0.05 g TNTs-Cl, reaction time 120 min.

increase in the values of  $\alpha$ -pinene conversion, which rose from 40.2% (100 °C) to 98.7% (110 °C). The highest selectivity of camphene was amounted to *ca.* 78.5% at 120 °C. The reaction temperature was further increased, while the selectivity of camphene was lowered. The result can be most probably

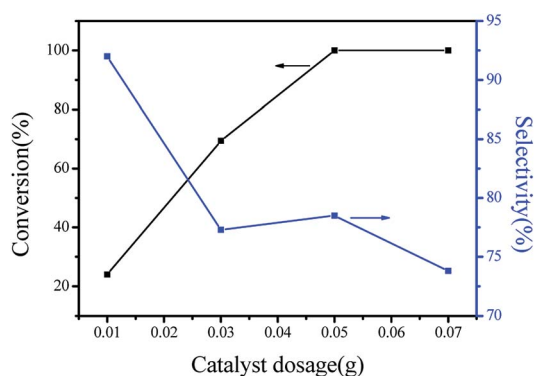


Fig. 6 Effect of the catalyst dosage on the  $\alpha$ -pinene conversion and camphene selectivity. Reaction conditions: 1 mL  $\alpha$ -pinene, reaction time 120 min, reaction temperature 120 °C.

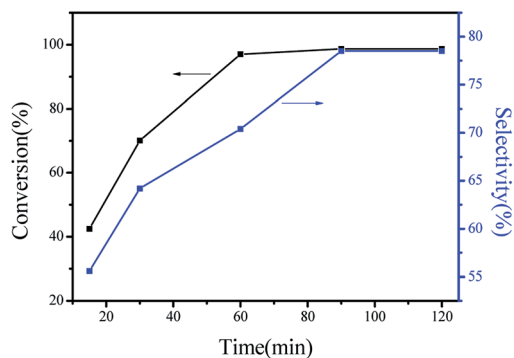


Fig. 7 Effect of reaction time on the  $\alpha$ -pinene conversion and camphene selectivity. Reaction conditions: 1 mL  $\alpha$ -pinene, 0.05 g TNTs-Cl, reaction temperature 120 °C.

explained by camphene transformed into monocyclic isomer products at relatively high temperature.

The effects of the catalyst dosage on the isomerization were further investigated, and the results are summarized in Fig. 6. It can be obviously seen that an increase in the catalyst amount resulted in the better catalytic performance in term of  $\alpha$ -pinene conversion. However, camphene selectivity remarkably decreased with the catalyst amount increase. This may be caused by the large amount of acidic active centers available, thus leading to higher production of monocyclic products. This phenomenon is in good agreement with results previously published.<sup>27</sup>

The effects of reaction time on the isomerization were investigated, and results are presented in Fig. 7. The conversion of  $\alpha$ -pinene increased with reaction time. However, the reaction rate was very slow after 60 min as if pseudo-equilibrium was reached. The conversion of  $\alpha$ -pinene remained 97.8% and the prolongation of the reaction time did not seem to increase obviously the system's activity. It is worth noting that camphene selectivity increases with the reaction time. After 90 min of reaction, camphene selectivity remained approximately unchanged, keeping at 78.5%.

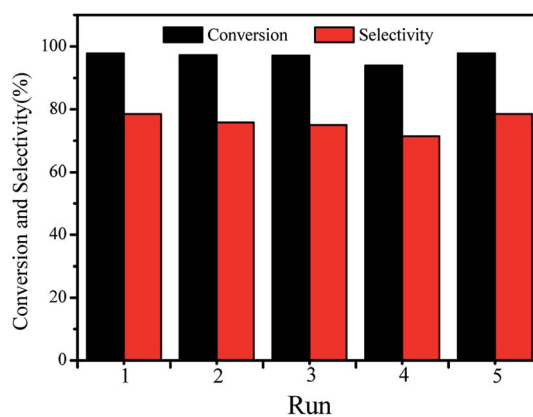


Fig. 8 Recycling of TNTs-Cl for the isomerization of  $\alpha$ -pinene. Reaction conditions: 1 mL  $\alpha$ -pinene, reaction time 120 min, 0.05 g TNTs-Cl, reaction temperature 120 °C.

Table 2 Comparison of TNTs-Cl with reported catalyst

Catalyst	Temp. (°C)	Time (h)	Cat./ $\alpha$ -pinene (wt%)	Conv. (%)	Camphene sele. (%)	Ref.
Zeolites beta	70	0.5	6	91.4	43.9	3
40Ga-41	80	1	3.5	61.0	65.0	27
H <sub>3</sub> PW <sub>12</sub> O <sub>40</sub> /SiO <sub>2</sub>	100	1	0.6	90.0	50.0	11
Sulfated zirconia	120	2	1.5	88.2	67.4	28
W <sub>2</sub> O <sub>3</sub> /Al <sub>2</sub> O <sub>3</sub>	150	2	1	73.0	55.0	10
Sulfated ZrO <sub>2</sub> -SiO <sub>2</sub>	150	2	5	98.0	34.0	29
Illite clay	140	1.6	1	85.0	54.3	7
Fe <sup>3+</sup> -loaded clinoptilolite	155	8	17	93.7	65.6	2
[HO <sub>3</sub> S-(CH <sub>2</sub> ) <sub>3</sub> -Net <sub>3</sub> ]Cl-ZnCl <sub>2</sub>	140	4	—	97.6	64.8	12
Ti-SBA-15	140	5	15	60.0	65.0	30
TNTs-Cl	120	2	5.8	97.8	78.5	This work

### Catalyst stability

The stability of TNTs-Cl was also evaluated during the isomerization process. After each run, TNTs-Cl was easily removed from the reaction mixture by centrifugation. The catalyst was washed and centrifuged repeatedly with hexane and ethanol to remove the residues. Then, the catalyst was reused in the next run. Fig. 8 shows that the catalyst exhibits fairly outstanding stability. The conversion of  $\alpha$ -pinene was maintained 94% with 71.4% camphene selectivity after four runs. While supplemental addition of 10% TNTs-Cl dosage for the mass lost in recovering, the conversion and selectivity in fifth are comparable to the first run. This indicates that the catalytic activity of TNTs-Cl catalyst was not much affected on recycling. The catalytic activities of various catalysts that have been studied in the previous literatures are summarized in Table 2. The catalysts with stronger acid sites, such as zeolites beta, H<sub>3</sub>PW<sub>12</sub>O<sub>40</sub>/SiO<sub>2</sub>, and sulfated ZrO<sub>2</sub>-SiO<sub>2</sub> have been reported for the isomerization of  $\alpha$ -pinene with low selectivity to camphene. The higher selectivity to camphene was achieved for 40Ga-41, sulfated zirconia, Fe<sup>3+</sup>-loaded clinoptilolite and Ti-SBA-15. It is worth noting that the catalytic performance of TNTs-Cl in the present work was better than that of other systems. These results indicate that TNTs-Cl worked as an acid catalyst exhibiting excellent catalytic performance in selective isomerization of  $\alpha$ -pinene to camphene.

### Conclusions

In conclusion, titanate nanotubes prepared by hydrothermal reconstitution and post-modification with HCl aqueous solution were studied in  $\alpha$ -pinene isomerization showing high selectivity to camphene (78.5% at 97.8%  $\alpha$ -pinene conversion). This catalyst exhibited outstanding catalytic performance and have an excellent stability over four runs. The study demonstrated that titanate nanotubes worked as an efficient solid acid catalyst for the green conversion of  $\alpha$ -pinene into value-added chemicals. Further works on the relationships between the strength of acid sites and the catalytic performances of titanate nanotubes are underway.

### Conflicts of interest

There are no conflicts to declare.

### Acknowledgements

This work was supported by the National Natural Science Foundation of China (Grant No. 21776068, 21606082), the Key Scientific Research Fund of Hunan Provincial Education Department (Grant No. 19A035) and Collaborative Innovation Center of New Chemical Technologies for Environmental Benignity and Efficient Resource Utilization.

### Notes and references

- 1 L. T. Mika, E. Cséfalvay and . Németh, *Chem. Rev.*, 2018, **118**, 505–613.
- 2 M. Akgül, B. zyağcı and A. Karabakan, *J. Ind. Eng. Chem.*, 2013, **19**, 240–249.
- 3 F. Tian, Y. Wu, Q. Shen, X. Li, Y. Chen and C. Meng, *Microporous Mesoporous Mater.*, 2013, **173**, 129–138.
- 4 X. Wang, L. Chen, D. Huang, J. Yue, Z. Luo and T. Zeng, *Catal. Lett.*, 2018, **148**, 3492–3501.
- 5 N. Kumar, P. Mäki-Arvela, S. F. Diáz, A. Aho, Y. Demidova, J. Linden, A. Shepidchenko, M. Tenhu, J. Salonen, P. Laukkanen, A. Lashkul, J. Dahl, I. Sinev, A.-R. Leino, K. Kordas, T. Salmi and D. Y. Murzin, *Top. Catal.*, 2013, **56**, 696–713.
- 6 A. I. M. Rabe, L. J. Durndell, N. E. Fouad, L. Frattini, M. A. Isaacs, A. F. Lee, G. A. H. Mekhemer, V. C. D. Santos, K. Wilson and M. I. Zaki, *Mol. Catal.*, 2018, **458**, 206–212.
- 7 A. Y. Sidorenko, A. Aho, J. Ganbaatar, D. Batsuren, D. B. Utenkova, G. M. Sen'kov, J. Wärnä, D. Y. Murzin and V. E. Agabekov, *Mol. Catal.*, 2017, **443**, 193–202.
- 8 J.-J. Zou, N. Chang, X. Zhang and L. Wang, *ChemCatChem*, 2012, **4**, 1289–1297.
- 9 J. Wang, W. Hua, Y. Yue and Z. Gao, *Bioresour. Technol.*, 2010, **101**, 7224–7230.
- 10 F. Tzompantzi, M. Valverde, A. Pérez, J. L. Rico, A. Mantilla and R. Gómez, *Top. Catal.*, 2010, **53**, 1176–1178.
- 11 K. A. D. S. Rocha, P. A. Robles-Dutenhefner, I. V. Kozhevnikov and E. V. Gusevskaya, *Appl. Catal., A*, 2009, **352**, 188–192.
- 12 Y. Liu, L. Li and C. X. Xie, *Res. Chem. Intermed.*, 2016, **42**, 559–569.

- 13 M. Hosseini-Sarvari, H. Sharghi and S. Etemad, *Chin. J. Chem.*, 2007, **25**, 1563–1567.
- 14 M. L. Kantam, S. Laha, J. Yadav and B. Sreedhar, *Tetrahedron Lett.*, 2006, **47**, 6213–6216.
- 15 D. Nguyen Thanh, O. Kikhtyanin, R. Ramos, M. Kothari, P. Ulbrich, T. Munshi and D. Kubička, *Catal. Today*, 2016, **277**, 97–107.
- 16 M. Z. Kassae, R. Mohammadi, H. Masrouri and F. Movahedi, *Chin. Chem. Lett.*, 2011, **22**, 1203–1206.
- 17 P. L. Anandgaonker, S. Jadhav, S. T. Gaikwad and A. S. Rajbhoj, *J. Cluster Sci.*, 2014, **25**, 483–493.
- 18 M. Hosseini-Sarvari, *Tetrahedron*, 2008, **64**, 5459–5466.
- 19 F. Shirini, S. V. Atghia and M. Alipour Khoshdel, *Iran. J. Catal.*, 2011, **1**, 93–97.
- 20 M. Golets, S. Ajaikumar and J.-P. Mikkola, *Chem. Rev.*, 2015, **115**, 3141–3169.
- 21 M. Kitano, K. Nakajima, J. N. Kondo, S. Hayashi and M. Hara, *J. Am. Chem. Soc.*, 2010, **132**, 6622–6623.
- 22 S. Zhou, X. Liu, J. Lai, M. Zheng, W. Liu, Q. Xu and D. Yin, *Chem. Eng. J.*, 2019, **361**, 571–577.
- 23 J. Guo, D. Yin and J. Guo, *J. Xiangtan. Nor. Univ., (Nat. Sci. Ed.)*, 2001, **23**, 65–68.
- 24 B. Rajendra Prasad Reddy, P. Vasu Govardhana Reddy and B. N. Reddy, *New J. Chem.*, 2015, **39**, 9605–9610.
- 25 W. Linghu, Y. Sun, H. Yang, K. Chang, G. Sheng, T. Hayat, N. S. Alharbi and J. Ma, *J. Mol. Liq.*, 2017, **244**, 146–153.
- 26 T. A. Silva, J. Diniz, L. Paixão, B. Vieira, B. Barrocas, C. D. Nunes and O. C. Monteiro, *Solid State Sci.*, 2017, **63**, 30–41.
- 27 R. Luque, J. M. Campelo, T. D. Conesa, D. Luna, J. M. Marinas and A. A. Romero, *Microporous Mesoporous Mater.*, 2007, **103**, 333–340.
- 28 N. A. Comelli, E. N. Ponzi and M. I. Ponzi, *Chem. Eng. J.*, 2006, **117**, 93–99.
- 29 K. B. Sidhpuria, B. Tyagi and R. V. Jasra, *Catal. Lett.*, 2011, **141**, 1164–1170.
- 30 A. Wróblewska, P. Miądlicki and E. Makuch, *React. Kinet., Mech. Catal.*, 2016, **119**, 641–654.